Development and application of 2.5 GPa-25 T high-pressure high-field electron spin resonance system using a cryogen-free superconducting magnet

Sakurai, T. ; Kimura, S. ; Kimata, M. ; Nojiri, H. ; Awaji, S. ; Okubo, S. ; Ohta, H. ; Uwatoko, Y. ; Kudo, K. ; Koike, Y.

(Citation)
Journal of Magnetic Resonance, 296:1-4

(Issue Date)
2018-11

(Resource Type)
journal article

(Version)
Accepted Manuscript

Development and Application of 2.5 Gigapascal-25 Tesla High-Pressure High-Field Electron Spin Resonance System using a Cryogen-Free Superconducting Magnet

T. Sakurai[a], S. Kimura[b], M. Kimata[b], H. Nojiri[b], S. Awaji[b], S. Okubo[c], H. Ohta[c], Y. Uwatoko[d], K. Kudo[e], Y. Koike[f]

[a] *Research Facility Center for Science and Technology, Kobe University, Nada, Kobe 657-8501, Japan*
[b] *Institute for Materials Research, Tohoku University, Sendai 980-8577, Japan*
[c] *Molecular Photoscience Research Center, Kobe University, Nada, Kobe 657-8501, Japan*
[d] *Institute for Solid State Physics, University of Tokyo, Chiba 277-8581, Japan*
[e] *Research Institute for Interdisciplinary Science, Okayama University, Okayama 700-8530, Japan*
[f] *Department of Applied Physics, Tohoku University, Sendai 980-8579, Japan*

Abstract

We have developed a high-pressure electron spin resonance probe and successfully installed into the world's highest-field cryogen-free superconducting magnet having a maximum central field of 24.6 T. The high pressure of 2.5 GPa is achieved by the specially designed piston-cylinder pressure cell using THz-wave-transparent components. In the first application of this high-pressure high-field ESR system, we observed that the orthogonal dimer spin system $SrCu_2(BO_3)_2$ undergoes a quantum phase transition from the dimer singlet ground to the plaquette singlet ground states.

Keywords: ESR, high pressure, high magnetic field, cryogen-free superconducting magnet, $SrCu_2(BO_3)_2$, quantum phase transition

1. Introduction

High-pressure high-field electron spin resonance (ESR) has been recognized recently as a powerful means to study magnetic materials [1]. Applying high field and/or high pressure may tune the competing magnetic energy levels and consequently induce the novel magnetic phases in materials, especially, strongly correlated spin systems.

In the ESR measurements, the highest pressure reached was 10 GPa at an X-band (10 GHz) system [2], whose corresponding resonance field is 0.36 T for a g-factor of $g = 2$. In this system, a diamond anvil cell (DAC), which is a device used to generate the very highest pressures, was used. The DAC was incorporated into the X-band system and the gasket acts as a resonant antenna. As the resonant structure needs to be scaled down to the wavelength of the corresponding electromagnetic wave in principle, the setup used in this X-band system cannot be simply applied to the high-frequency region. Another DAC technique is used in the high-field ESR system with high magnetic field of up to 4 T [3]. In Ref. [3] a plastic DAC was developed that can be set into the cavity which operates in the frequency region 40 -160 GHz. However, the use of plastics restricts the pressure to 2.2 GPa.

We have developed a piston-cylinder pressure cell for the high-field ESR, which produces the highest pressure of up to 2.5 GPa among the high-field ESR systems [1, 4]. We used a double-layer cylinder consisting of an inner NiCrAl cylinder and an outer CuBe sleeve, enabling pressures of up to 2.5 GPa beyond the upper limits of a single-layer cylinder. We also used ceramics as inner parts and they allowed for electromagnetic-wave transmission in THz region. In addition, because in our system a simple transmission method is used, the frequency of the electromagnetic wave can be continuously varied up to 800 GHz in contrast to the cavity-type ESR system. Although the sensitivity is not as high as compared with that using the cavity method or the system using quasi-optical method [5], its large sample space ($4\phi \times \sim 10$ mm) enables us a relatively high signal-to-noise ratio.

The highest field in the high-pressure ESR measurements was achieved by combining a 55-T pulsed magnet with our piston-cylinder pressure cell and electromagnetic wave transmission setup [6]. However, the maximum pressure was 1 GPa at most because only a single-layer cylinder was available as the inner magnet bore was small. Although ESR measurements at further extreme conditions may become possible using a wide-inner-bore pulsed magnet [7], several difficult problems caused by the eddy currents occurring during the pulse field application on the pressure cell, which is made of metal alloy [8], have to be solved.

Extending both the magnetic field and pressure ranges simultaneously is still challenging. Here we describe a new high-pressure ESR system by combining our original wide-frequency coverage 2.5-GPa pressure cell with the world's highest-field cryogen-free superconducting magnet (hereinafter called the 25T-CSM) installed recently at Institute for Materials Research (IMR), Tohoku University [9]. Its maximum field is 24.6 T, which is unobtainable by any commercially available superconducting magnet. By this ESR system, we are able to perform ESR measurements that have never been done before with the prospect of discovering novel physical phenomena in-

Email address: tsakurai@kobe-u.ac.jp (T. Sakurai)

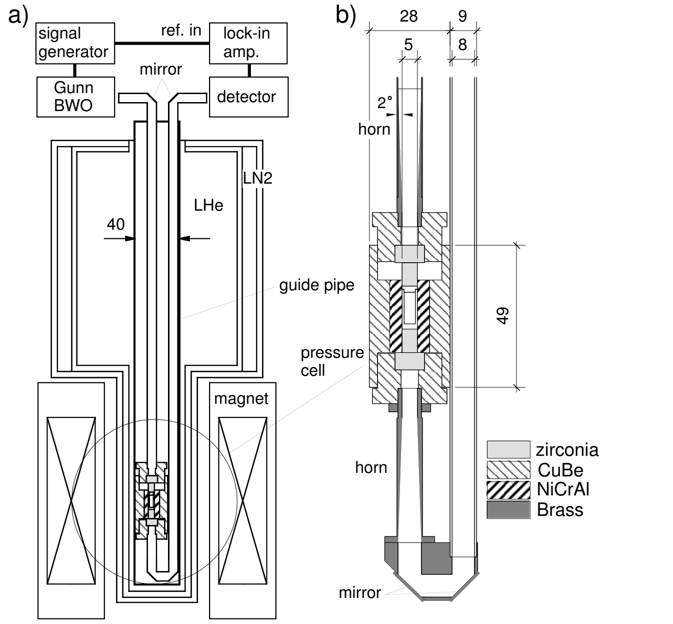

Figure 1: a) Schematic diagram of the high-pressure ESR system using the 25-T cryogen-free superconducting magnet; b) Enlarged view for the pressure cell and the bottom mirrors. The inner and outer diameters of the pressure cell are 5 mm and 28 mm, respectively.

duced by such high-pressure and high-field conditions. Indeed, we demonstrate an interesting phase transition observed using this newly developed high-pressure high-field ESR system in this article. We also present the outline of our new system.

2. Outline of high-field high-pressure ESR system

In our previous high-pressure ESR system, the transmitted electromagnetic wave passing through the pressure cell is detected by the InSb hot-electron bolometer set below the pressure cell [4]. Although a straight path from the pressure cell to the detector is favored for a low-loss propagation of the electromagnetic wave, such detector arrangement requires a special cryostat that has sufficient depth below the magnet because the detector loses the sensitivity in the high field. In this study we modified the design to fit more general cryostats. With the designed ESR probe (Fig. 1), the pressure cell is located at the center of the magnet. The transmitted electromagnetic wave is reflected by two sets of mirrors at each end of the light pipe set above and below the pressure cell. Each mirror reflects the electromagnetic waves through 90°. The inner and outer diameters of the pressure cell are 5 mm and 28 mm, respectively. Although the inner diameter of the pressure cell corresponds to the cutoff frequency of 60 GHz, we can observe the transmitted intensity with the lower frequency because ZrO_2-based ceramics used as inner parts of the pressure cell is expected to have a relatively high dielectric constant. Indeed, we observed ESR signal at 50 GHz as is mentioned in next section. The inner diameter of the light pipe are 8 mm and the top and bottom of the pressure cell are connected to the light pipe through tapered horns. The whole probe, with a total length of 1800 mm, is inserted into a 40-mm-diameter insert pipe chamber filled with He exchange gas. The present probe can fit into not only the 25T-CSM but also the standard superconducting magnet with 50-mm cold bore.

The pressure is generated by the pressure cell, which is similar to that developed for THz ESR [4]. The key feature of this pressure cell is that all its inner parts are made of ZrO_2-based ceramics. These ceramics are both tough and transparent to electromagnetic waves, enabling both high pressures of up to 2.5 GPa and a wide range of frequencies, 50-800 GHz, to be available in applications. Details of this pressure cell can be found in Refs. [4, 10, 11].

Gunn oscillators and backward wave oscillators (BWOs) are used as the light sources. The light pipes for the incident and transmitted electromagnetic waves are typically about 2 m in length. The intensity of the electromagnetic wave from these light sources can be modulated electrically. The transmitted electromagnetic wave is detected using commercially available InSb detector (QFI/2BI, QMC Instruments Ltd.) or Schottky diode detector set outside of the cryostat and amplified by a lock-in amplifier using a modulation frequency as a reference signal. The intensity of the electromagnetic wave is reduced at mirrors and along the lengthy paths probably to one tenth or less of the previous system [4]. However, an InSb detector used in the previous system is home-made and less sensitive. Consequently, the high sensitivity of commercially available detectors compensates the intensity losses in this system and we obtain a similar signal-to-noise ratio with the previous one.

The 25T-CSM at the IMR Tohoku University has been open since 2017 as a multiuse magnet. This magnet consists of an inner $Bi_2Sr_2Ca_2Cu_3O_y$ (Bi2223) high-T_c coil, and a middle Nb_3Sn and an outer NbTi low-T_c coils [9]. Both high- and low-T_c superconducting magnets are charged or discharged simultaneously. The maximum field of 24.6 T in the background field of 14 T generated by low-T_c coils is achieved in a 52 mm room-temperature bore with one-hour ramping time. This is the highest field value among those produced by cryogen-free superconducting magnets. For details, see Ref. [9]. For measurements below liquid He temperature, a cryostat with an inner diameter of 44 mm is available.

3. Application to orthogonal dimer spin system $SrCu_2(BO_3)_2$

As the first application example, we present the results for the orthogonal dimer spin system $SrCu_2(BO_3)_2$. $SrCu_2(BO_3)_2$ has a unique spin arrangement known as the Shastry-Sutherland lattice [12]. The Cu^{2+} dimers are arranged orthogonally to each other in the *ab*-plane, as shown in Fig. 2 (a). They form an $S = 1/2$ two-dimensional network through the antiferromagnetic intradimer (indicated by solid line) and interdimer (dashed line) exchange interactions. The ground state of this compound is the product of dimer singlet state. There is a significant competition between intradimer and interdimer exchange interactions and this results in the strong spin frustration within

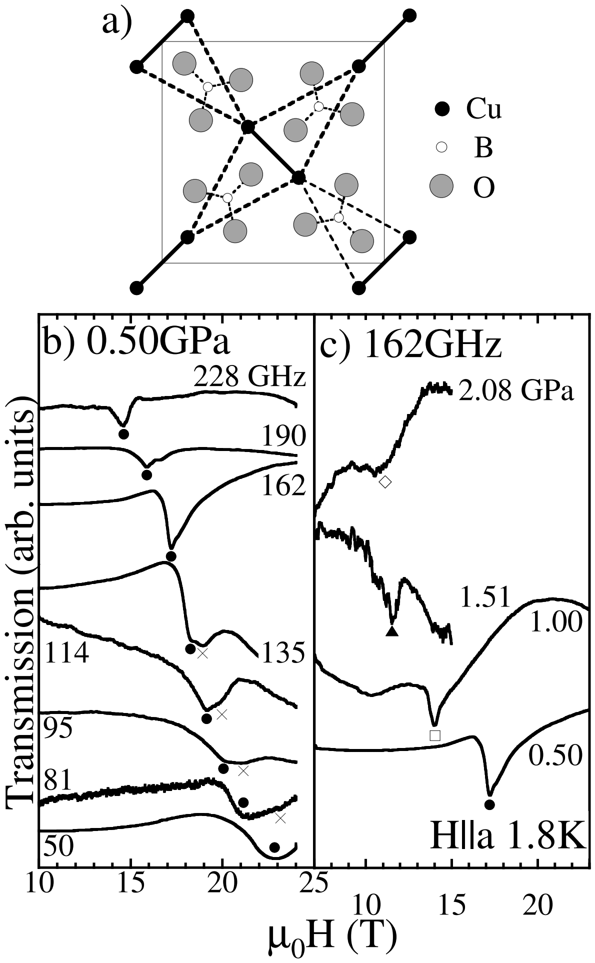

Figure 2: Crystal structure of $SrCu_2(BO_3)_2$ in the *ab*-plane (a) and typical ESR spectra obtained under pressures for H||a and 1.8 K (b, c): (b) frequency-dependent spectra obtained at 0.50 GPa and (c) pressure-dependent spectra obtained at 162 GHz. Symbols indicate peak positions.

the system. Above the critical value for the ratio of the interdimer to the intradimer exchange interactions, the system is predicted to have the plaquette singlet ground state [13]. Moreover, the ratio of the system is expected to be close to this critical value and pressure has the potential to tune this ratio. However, because this quantum phase transition is a nonmagnetic-nonmagnetic transition, it is difficult to distinguish it by only measuring a macroscopic quantities such as the magnetic susceptibility. In theory, this transition is a first-order phase transition accompanied with a discontinuous change in the excitation energies from the ground state to the triplet states at the critical point [14]. As the high-field ESR measurements observed the excited states very clearly for this system [15], such measurements at high pressure offer a means to investigate this phase transition. Recently, within the field range of 10 T, we revealed that the system undergoes a quantum phase transition at 1.85 GPa [16]. On the other hand, the first excited triplet states cross the ground state at around 25 T at 0 GPa [15]. Therefore, the high-pressure ESR measurements using 25T-CSM is expected

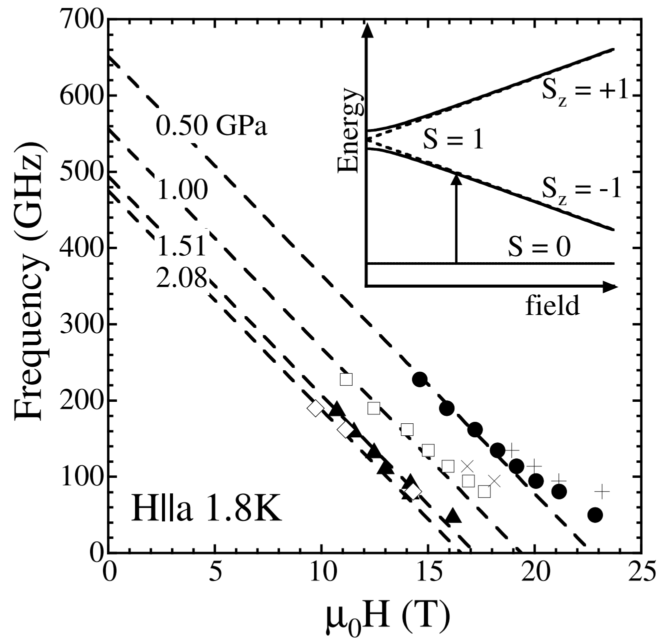

Figure 3: Frequency-field diagram of $SrCu_2(BO_3)_2$ obtained at various pressures. The broken lines are the linear fitting results. The inset shows the schematic energy-field diagram. The solid and dotted lines show the theoretical lines given in the text and their asymptotes $h\nu = j \pm g\mu_B H$, respectively.

to add further details of the quantum phase transition through this level crossing.

In this experiment, several Gunn oscillators cover the frequency range from 50 to 228 GHz. Figure 2 (b) and (c) show typical ESR spectra obtained at various frequencies and pressures. We succeeded in observing ESR of $SrCu_2(BO_3)_2$ up to 2.08 GPa in the field range of 24.0 T. Even at 50 GHz, which is lower than the cutoff frequency corresponding to the inner diameter of the pressure cell (5 mm, 60 GHz), we obtained the ESR signal with a good signal-to-noise ratio. The frequency-field diagram at various pressures (Fig. 3) shows that the resonance field approaches a straight line with a constant slope when the frequency is increased. A comparison of the results obtained at ambient pressure [15] indicates that the observed signals (see inset) turns out to correspond to transitions from the ground state ($S = 0$) to the $S_z = -1$ state of the excited triplet states ($S = 1$). The broken lines in Fig. 3 are fits with $g = 2.05$ [15] for the frequency region $\nu \geq 135$ GHz. The intercepts at zero field are the gap energies between the singlet ground state and the triplet states. Moreover, the gap energy (Fig. 4) decreases with increasing pressure below 1.51 GPa but does not change much across the transition point 1.85 GPa. Figure 2 (c) demonstrates this tendency very clearly; the resonance position shifts to lower fields as pressure is applied in the region below 1.51 GPa, whereas it does not change much from 1.51 to 2.08 GPa.

In Fig. 4, the gap energies obtained in previous ESR measurements with the field range below 10 T and the frequency range up to 800 GHz [16] are also shown. They show a clear

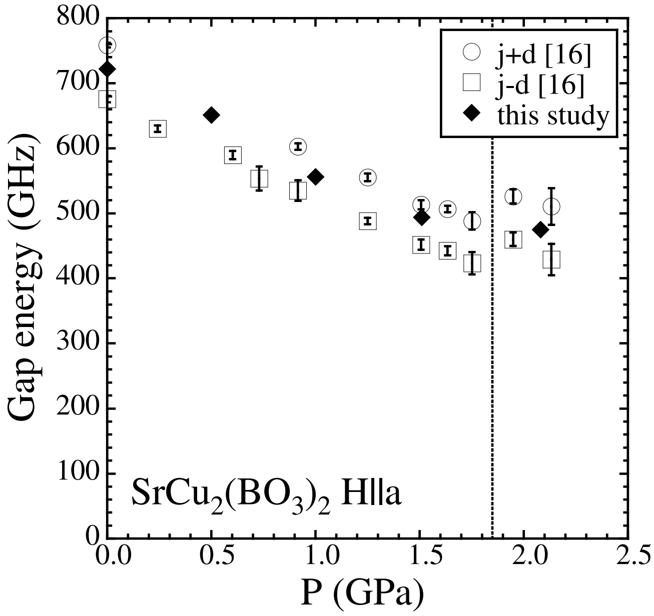

Figure 4: Pressure dependence of the gap energy of $SrCu_2(BO_3)_2$ for H||a and 1.8 K (filled diamonds). Data indicated by open symbols are taken from Ref. [16].

discontinuous change at 1.85 GPa. From the detailed analysis using an exact diagonalization, we concluded that this discontinuous change corresponds to the quantum phase transition from the dimer singlet state to the plaquette singlet state [16]. Except around the crossing field, the gap energy follows an effective equation $h\nu = j \pm \sqrt{d^2 + (g\mu_B H)^2}$, where h is the Planck constant, μ_B is the Bohr magneton, and j and d are fitting parameters [17]. Under conditions of previous experiments, the zero-field splittings corresponding to the quantities $j \pm d$ were obtained, whereas in this study the gap energies were only approximately determined; see the schematic in the inset of Fig. 3. Nevertheless, the obtained pressure dependence of the gap energy in this study reproduces the previous results consistently across the quantum phase transition. The reason why we obtain a small change in the gap energy between 1.51 and 2.08 GPa in this study is because the gap energy at 1.51 GPa in the dimer singlet phase is accidentally close to that at 2.08 GPa in the plaquette singlet phase.

As shown in Fig. 2 (b), the absorption line seems to be broadened as the frequency is decreased. This is because the absorption line is split as indicated by a circle and a cross and the splitting width increases as the frequency is decreased. The similar behavior is also observed at ambient pressure clearly [15]. The deviation from the straight line with decreasing the frequency can also be seen at 0.50 GPa as shown in Fig. 3. These splitting and anticrossing were also observed at 1.00 GPa, whereas they were not observed clearly at 1.51 and 2.08 GPa (Fig. 3). The intradimer Dzyaloshinsky-Moirya (DM) interaction may cause these splitting and anticrossing [18]. Therefore, the intradimer DM interaction is expected to be weakened by pressure. In previous study, although we did not obtain the pressure dependence of the intradimer DM interaction directly, we determined that of the intradimer exchange interaction. We found that it has a negative slope to the pressure (-7.4 %/GPa) [16]. If we assume that the intradimer DM interaction scales to the intradimer exchange interaction, it is reduced by 15 % at 2.08 GPa. However, further investigation is required to clarify whether these pressure effects can be explained quantitatively by solely the weakening of the DM interaction. On the other hand, the line broadening above the phase transition is very large [Fig. 2 (c)] in contrast to the gradual change seen in the anticrossing behavior. This abrupt change in the absorption line supports the occurrence of the phase transition from the dimer phase to the plaquette phase. Therefore, we conclude that the system undergoes this phase transition at 1.85 GPa.

4. Summary

A high-pressure ESR probe was developed for the 25T-CSM, the world's highest-field cryogen-free superconducting magnet. Pressure is generated by a double-layer piston-cylinder pressure cell and capable of a maximum pressure of 2.5 GPa. This pressure cell uses ceramics as its inner parts which enables us to observe the transmitted electromagnetic wave in the frequency region from 50 to 800 GHz. When this probe is combined with the 25T-SCM, we are able to explore novel physical phenomena by ESR measurements under unrivaled high-pressure and high-field conditions. We applied this high-pressure high-field ESR system to study the orthogonal dimer spin system $SrCu_2(BO_3)_2$ in the pressure range up to 2.1 GPa and succeeded in observing the quantum phase transition from the dimer singlet state to the plaquette singlet state.

Acknowledgments

This work was performed under the Inter-university Cooperative Research Program of the Institute for Materials Research, Tohoku University (Proposal Nos. 16H0001, 17H0040, 18H0020). This research was also partially supported by Grants-in-Aid for Scientific Research (C) (No. 16K05416) from Japan Society for the Promotion of Science.

[1] T. Sakurai, S. Okubo, H. Ohta, High-field/high-pressure ESR, J. Magn. Reson. **280** (2017) 3-9.

[2] N. Sakai, J. H. Pifer, Electron paramagnetic resonance at high pressure using a diamond anvil cell, Rev. Sci. Instrum. **56** (1985) 726

[3] K. Thirunavukkuarasu, S. M. Winter, C. C. Beedle, A. E. Kovalev, R. T. Oakley, S. Hill, Pressure dependence of the exchange anisotropy in an organic ferromagnet, Phys. Rev. B **91** (2015) 014412

[4] T. Sakurai, K. Fujimoto, R. Matsui, K. Kawasaki, S. Okubo, H. Ohta, K. Matsubayashi, Y. Uwatoko, H. Tanaka, Development of multi-frequency ESR system for high-pressure measurements up to 2.5 GPa, J. Magn. Reson. **259** (2015) 108

[5] B. Náfrádi, R. Gaál, A. Sienkiewicz, T. Fehér, L. Forró, Continuous-wave far-infrared ESR spectrometer for high-pressure measurements, J. Magn. Reson. **195** (2008) 206

[6] T. Sakurai, M. Tomoo, S. Okubo, H. Ohta, K. Kudo, Y. Koike, High-field and high-pressure ESR measurements of $SrCu_2(BO_3)_2$, J. Phys.: Conf. Ser. **150** (2009) 0242171.

[7] M. Hagiwara, T. Kida, K. Taniguchi, K. Kindo, Present Status and Future Plan at High Magnetic Field Laboratory in Osaka University, J. Low. Temp. Phys. **170** (2013) 531
[8] T. Sakurai, A. Taketani, T. Tomita, S. Okubo, H. Ohta, Y. Uwatoko, Development of high-pressure, high-field and multifrequency electron spin resonance system, Rev. Sci. Instrum. **78** (2007) 065107.
[9] S. Awaji, K. Watanabe, H. Oguro, H. Miyazaki, S. Hanai, T. Tosaka, S. Ioka, First performance test of a 25 T cryogen-free superconducting magnet, Supercond. Sci. Technol. **30** (2017) 065001
[10] H. Ohta,,T. Sakurai, R. Matsui, K. Kawasaki, Y. Hirao, S. Okubo, K. Matsubayashi, Y. Uwatoko, K. Kudo, and Y. Koike, Frequency Extension to THz Range in High Pressure ESR System and Its Application to Shastry-Sutherland Model Compound $SrCu_2(BO_3)_2$, J. Phys. Chem. B **119** (2015) 13755
[11] T. Sakurai, R. Matsui, K. Kawasaki, S. Okubo, H. Ohta, K. Matsubayashi, Y. Uwatoko, K. Kudo, Y. Koike, Development of High-Pressure and Multi-Frequency ESR System and Its Application to Quantum Spin System, Appl. Mag. Res. **46** (2015) 1007
[12] H. Kageyama, K. Yoshimura, R. Stern, N. V. Mushnikov, K. Onizuka, M. Kato, K. Kosuge, C. P. Slichter, T. Goto, Y. Ueda, Exact Dimer Ground State and Quantized Magnetization Plateaus in the Two-Dimensional Spin System $SrCu_2(BO_3)_2$, Phys. Rev. Lett. **82** (1999) 3168.
[13] S. Miyahara, K. Ueda, Exact Dimer Ground State of the Two Dimensional Heisenberg Spin System $SrCu_2(BO_3)_2$, Phys. Rev. Lett. **82** (1999) 3701.
[14] Y. Takushima, A. Koga, N. Kawakami, Competing Spin-Gap Phases in a Frustrated Quantum Spin System in Two Dimensions, J. Phys. Soc. Jpn. **70** (2001) 1369.
[15] H. Nojiri, H. Kageyama, K. Onizuka, Y. Ueda, M. Motokawa, Direct Observation of the Multiple Spin Gap Excitations in Two-Dimensional Dimer System $SrCu_2(BO_3)_2$, J. Phys. Soc. Jpn. **68** (1999) 2906. H. Nojiri, H. Kageyama, Y. Ueda, M. Motokawa, ESR Study on the Excited State Energy Spectrum of $SrCu_2(BO_3)_2$, J. Phys. Soc. Jpn. **72** (2003) 3243.
[16] T. Sakurai, Y. Hirao, K. Hijii, S. Okubo, H. Ohta, Y. Uwatoko, K. Kudo, Y. Koike, Direct Observation of the Quantum Phase Transition of $SrCu_2(BO_3)_2$ by High-Pressure and Terahertz Electron Spin Resonance, J. Phys. Soc. Jpn. **87** (2018) 033701.
[17] O. Cépas, K. Kakurai, L. P. Regnault, T. Ziman, J. P. Boucher, N. Aso, M. Nishi, H. Kageyama, and Y. Ueda, Dzyaloshinski-Moriya Interaction in the 2D Spin Gap System $SrCu_2(BO_3)_2$, Phys. Rev. Lett. **87** (2001) 167205.
[18] S. El Shawish, J. Bonča, C. D. Batista, and I. Sega, Electron spin resonance of $SrCu_2(BO_3)_2$ at high magnetic fields, Phys. Rev. B **71** (2005) 014413.